

INTERPRETING PALEOHYDROLOGY AND FLUVIAL DYNAMICS OF MARTIAN CHANNELS IN THE AEOLIS DORSA REGION. C. E. Russell¹, K. Konsoer¹, S. Karunatilake¹, D. Burr² and A. Forte¹,
¹Louisiana State University (cr295@lsu.ac.uk), ²Northern Arizona University.

Introduction: Martian paleochannels can represent fluvial and paleoclimatic evolution^[1]. However, the dynamic nature of Mars' fluvial systems remains obscure because prior works generally focus on generalized interpretations and thresholds from paleochannels. Substantiated and detailed interpretations of these preserved deposits can be compared with studies of terrestrial systems, both modern and preserved^[2,3], and offer insight into interpreting their paleohydrologic variability and fluvial dynamics, such as meander planform evolution, relative rates of bend migration, and inferred spatial distribution of point bar sedimentology. Aeolis Dorsa (AD) (Fig. 1), is a region characterized as fluvially modified that displays exceptionally well-preserved fluvial morphologies including meander morphologies^[4-10], making it a ripe area for such analyses.

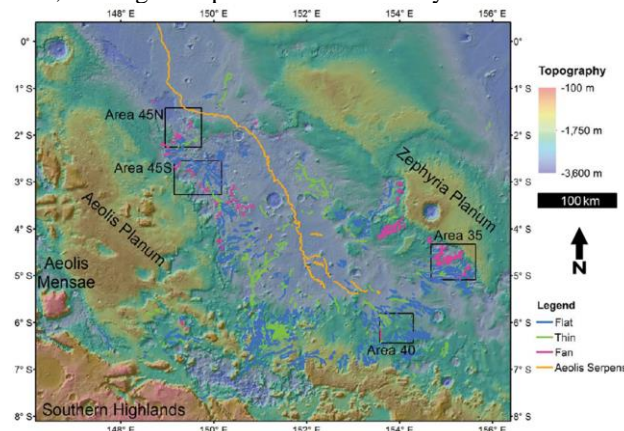


Fig. 1: Study area map of the Aeolis Dorsa region with over 1600 individual features delineated. Preliminary analyses of inverted channels shown in the Methods section below are from the area denoted by the black box of Area 40. Legend denotes different types of inverted channel morphologies. Modified from Jacobsen and Burr, 2017^[11].

Meander shape is influenced by controls such as: the size and gradation of transported sediment^[12,13] timing and frequency of meander-loop cut off^[14] bank material and variations in the erodibility of the floodplain^[15], the ratio of mean annual river discharge and meander wavelength^[16], and climate change^[17,18].

Scroll bar deposits are the remnants of an active and changing system preserved within the alluvial floodplain architecture^[19,20]. As a meandering river migrates through its floodplain, the growth and planform evolution of its meander bends result in lateral accretion along the point bar and formation of scroll bar topography, which records the migration

history of the river^[21,22]. Various combinations in growth result in complex planform deposits observed for natural meandering rivers. There is a spatial sorting of grain size whereby it becomes progressively finer in the downstream reaches of the point bar deposit^[23-25], and from understanding such processes, predictive methodologies have been produced^[26].

We aim to characterize the fluvial dynamics and paleochannel evolution characteristics at finer temporal resolution (i.e., annually to event-driven events) in Aeolis Dorsa as a case study for developing our techniques for broader application to inverted fluvial channels across Mars^[27]. We will apply interpretive and quantitative methods that we recently developed for meandering rivers on Earth, based on extensive observational datasets of meander planform geometries and patterns of scroll bar morphology^[26]. The results will be used to quantify the morphological variability of meandering channels, and to assess paleoflow direction and paleohydrologic variability, as well as paleo-fluvial dynamics, that may in turn be controlled by landscape characteristics. Where scroll bar patterns are observed we will also describe and characterize the temporal development of meander bends, and hence the mode by which the channels developed through an evolving climatic regime.

Methodology: Paleochannel planform geometry will be characterized using a refined approach of the Intersection Shape Method (ISM)^[26], which objectively classifies individual meander bends into 4 groups and 25 distinctive shapes. The methodology relies on quantitative metrics for characterizing the vast range of meandering river planform geometries that are observed in nature and has been successfully applied to 13 rivers from a range of environmental and climatic regions on Earth with a quantitative identification accuracy of 93%^[26]. Our preliminary work demonstrates the utility of interpretive fluvial mapping and ISM for Martian channels on an inverted, positive relief channel from the Aeolis Dorsa region (Fig. 2). This inverted paleochannel has a calculated length of over 5000 m, an average width of 50.6 m (ranging from 33.5 – 67.2 m), and a reach sinuosity of 1.45 (Fig. 2A-B) with morphologic evidence of meander scars and scroll bar morphologies, mapped with different colors as interpreted superposing chronological sequences (Fig. 2C).

Based on the ISM characterization, 8 of the 9 bends are classified as being within Group 4 – Open Symmetric, with Bend 9 being classified into Group 3 – Bulbous (Fig. 2B;^[26]). The presence of scroll bar morphologies and meander scars adjacent to the most prominent channel (Fig. 2B) offer additional information that may be drawn out through interpretive mapping. In Fig. 2C, the multiple identified channel paths depict that the most recent fluvial activity gave rise to a reach that was less sinuous than had occurred throughout its history (i.e., light blue channel exhibits lower sinuosity than others in the image). This fundamentally distinctive change in morphology may be representative of a climatic change. The presence of scroll bars in Fig. 2A suggests that flow was sustained, supporting the notion of a stable climate, or one with repeated or regular fluctuations. Many meander loops appear to have been abandoned prior to the limbs meeting and initiating neck cutoff, as is frequently seen on Earth in chute cut-off or avulsion dynamics^[28,29]. The difference in abandonment characteristics could be an indication of channel stability, and hence provide a morphometric comparison between terrestrial and Martian channels.

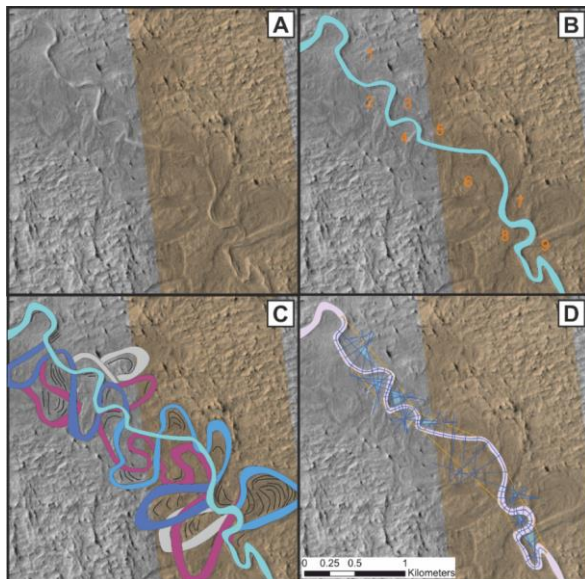


Fig. 2: Demonstration of preliminary work with the datasets that will be used in this study. Flow direction is determined as south to north via studying morphologies: A) original HiRISE image (ESP_034189_1740); B) Nine meanders defined in this reach through identifying tangents from the centerline of the channel^[26]; C) interpretive mapping of the reach, using meander scars to establish the chronological sequence as identified with colors on the image, oldest to youngest channels grade purple to light blue respectively; D) channel positions from which the metrics have been derived, which in turn enable the quantification of the meander shapes. The methodology referred to here, is the Intersection Shape Methodology^[26].

The wealth of quantified categorical information resulting from our tasks on planform morphological analyses will directly address not only the extent of sustained fluvial processes, but also enable additional insight on the precipitation regimes that supported them. Fundamentally, that insight will advance the ongoing discussion of the extent to which surface hydrology, especially fluvial systems, could have been sustained on ancient Mars despite a faint young Sun. Current works diverge on the underlying mechanisms of sustained fluvial systems as either basal melting of ice sheets from geothermal flux^[30] or sustained greenhouse conditions of the early Martian atmosphere^[31]. Additionally, understanding the relative influences of surface hydrology, basal melting of ice sheets, precipitation, and the Noachian groundwater table^[30,32,33], are critical questions that the morphological signals in this study may assist in determining answers for.

Acknowledgments: SK's participation supported by MDAP- 80NSSC18K1375.

References: ^[1] Kite, E.S. (2019) SSR, 215, 1-58. ^[2] Nanson, G.C. and Hickin, E.J. (1983) JHE, 109, 327-337. ^[3] Williams, R.M.E. et al., (2007) JGR:P, 112, 221-235. ^[4] Burr et al., (2009) Ic., 200, 52-76. ^[5] Burr et al., (2010) JGR, 115. ^[6] Zimelman, J.R., and Griffin, L.J. (2010) Ic., 205, 198-210. ^[7] Lefort, A. et al., (2012) JGR, 117. ^[8] Williams, R.M.E. et al., (2013) Ic., 225, 308-324. ^[9] Kite, E.S. et al., (2015) Ic., 253, 223-242. ^[10] Konsoer, K.M. et al., (2018) Geology, 46, 183-186. ^[11] Jacobsen, R.E. and Burr, D.M. (2017) Geosphere, 13, 2154-2168. ^[12] Allen, J.R.L. (1965) Sed., 5, 89-191. ^[13] Church, M. (2006) AREPS, 34, 325-354. ^[14] Lewis, G.W. and Lewin, J. (1983) SP IAS, 6, 145-154. ^[15] Jacobsen, R.E. and Burr, D.M. (2018) Ic., 302, 407-417. ^[16] Carlston, C.W. (1965) AJS, 263, 864-885. ^[17] Leopold, L.B. and Wolman, M.G. (1957) UGSG, PP 282-B, 39-84. ^[18] Alford, J.J. and Holmes, J.C. (1985) An. Assoc. American Geog., 75, 395-403. ^[19] Jackson, R.G. (1976) Sed., 23, 593-623. ^[20] Nanson, G.C. (1980) Sed., 27, 3-29. ^[21] Strick, R.J.P. et al., (2018) Geomorph., 310, 57-68. ^[22] Mason, J., and Mohrig, D. (2019) ESPL, 44, 2649-2659. ^[23] Labrecque, P.A. et al., (2011) Bull. of Can. Pet. Geo., 59, 147-171. ^[24] Fustic, M. et al., (2012) Mar. and Pet. Geol., 29, 219-232. ^[25] Durkin, P.R. et al., (2015) JSR, 85, 1238-1257. ^[26] Russell, C.E. et al., (2018) SP 48 IAS, 385-418. ^[27] Dickson, J.L. et al., (2020) 51st LPSC, 2326. ^[28] Constantine, J.A. et al., (2010) Sed., 57, 389-407. ^[29] Richards, D., and Konsoer, K.M. (2020) ESPL, 45, 1067-1081. ^[30] Ojha, L. et al., (2020) Sci. Adv., 6. ^[31] Deng et al. (2020) Sci. Adv., 6. ^[32] Galofre, A. G. et al., (2020) Nat. Geo. ^[33] Lingam, M., and Loeb, A. (2020) TAJ, 901, L11.